



DOI: 10.5604/01.3001.0015.3593

# Analytical and numerical free vibration analysis of porous functionally graded materials (FGPMs) sandwich plate using Rayleigh-Ritz method

E.K. Njim <sup>a</sup>, S.H. Bakhy <sup>a</sup>, M. Al-Waily <sup>b,\*</sup>

<sup>a</sup> Department of Mechanical Engineering, University of Technology, Baghdad, Iraq

<sup>b</sup> Department of Mechanical Engineering, Faculty of Engineering, University of Kufa, Kufa, Iraq

\* Corresponding e-mail address: muhanedl.alwaeli@uokufa.edu.iq

ORCID identifier:  <https://orcid.org/0000-0002-7630-1980> (M.A.-W.)

## ABSTRACT

**Purpose:** This study introduces a new approximated analytical solution of the free vibration analysis to evaluate the natural frequencies of functionally graded rectangular sandwich plates with porosities.

**Design/methodology/approach:** The kinematic relations are developed based on the classical plate theory (CPT), and the governing differential equation is derived by employing the Rayleigh-Ritz approximate method. The FGM plate is assumed made of an isotropic material that has an even distribution of porosities. The materials properties varying smoothly in the thickness direction only according to the power-law scheme.

**Findings:** The influences of changing the gradient index, porosity distribution, boundary conditions, and geometrical properties on the free vibration characteristics of functionally graded sandwich plates are analysed.

**Research limitations/implications:** A detailed numerical investigation is carried out using the finite element method with the help of ANSYS 2020 R2 software to validate the results of the proposed analytical solution.

**Originality/value:** The results with different boundary conditions show the influence of porosity distribution on the free vibration characteristics of FG sandwich plates. The results indicated a good agreement between the approximated method such as the Rayleigh-Ritz and the finite element method with an error percentage of no more than 5%.

**Keywords:** FGM sandwich plate, Porosity parameter, CPT, Free vibration, FEA

**Reference to this paper should be given in the following way:**

E.K. Njim, S.H. Bakhy, M. Al-Waily, Analytical and numerical free vibration analysis of porous functionally graded materials (FGPMs) sandwich plate using Rayleigh-Ritz method, Archives of Materials Science and Engineering 110/1 (2021) 27-41.

DOI: <https://doi.org/10.5604/01.3001.0015.3593>

## METHODOLOGY OF RESEARCH, ANALYSIS AND MODELLING

## 1. Introduction

Sandwich structures made of functionally graded materials (FGMs) have found widespread use in the automotive, marine construction, transportation, and aerospace industries due to their excellent bending rigidity, low specific weight, and distinct vibration characteristics [1]. Recently, a critical review of the fabrication, design, and application of FGM materials was introduced by Aman Garg et al. [2]. Many researchers have conducted static and dynamic analyses of FGM structures. Abderrahmane et al. [3] used refined shear deformation theory to examine the dynamic analysis of the functionally graded sandwich plate seated on an elastic foundation with three types of support. Irwan Katili et al. [4] used the finite element method (FEM) based on a discrete shear projection method to study static and free vibration analysis of FGM plates. Yang and Shen [5] investigated the dynamic response of initially stressed functionally graded rectangular thin plates subjected to partially distributed impulsive laterals and without or resting on an elastic foundation. By employing the variable shear deformation theory, a comprehensive study on the dynamic response of a functionally graded plate is presented in [6,7]. Jun Liu et al. [8] investigated free vibration and transient dynamic behaviours of FGM sandwich plates used semi-analytically by the scaled boundary finite element method. However, in the process of FGM manufacturing, the presence of porosity and micro-voids inside the materials possibly occurs due to technical problems.

Nuttawit and Variddhi [9] studied the influence of porosities on vibration analysis of elastically restrained ends of FGM beams, whereas Zhao et al. [10] studied free vibrations of a functionally graded porous rectangular plate with uniform elastic boundary conditions. Ismail Mechab et al. [11] examined the porosity impact on the free vibration of FGM nanoplates, which rested on a Winkler–Pasternak foundation. Yan Qing Wang and Jean W. Zu [12] presented a new mathematical model for the vibration behaviors of FGM plates with porosities subjected to thermal load. Farajollah et al. [13] investigated the free vibration analysis of functionally graded porous doubly-curved shells based on the first-order shear deformation theory. Prapot and Nuttawit [14] described flexural vibration analysis of FG sandwich plates resting on an elastic foundation with arbitrary boundary conditions; the governing equations of free vibration problems are derived from the first-order shear deformation theory that covers the essential effects of shear deformation and rotary inertia. Hassen et al. [15] presented a comprehensive study of free vibration analysis of porous FGM beams resting on an elastic foundation with two parameters.

Nuttawit Wattanasakulpong et al. [16] used the modified couple stress approach to study free vibration analysis of FGM sandwich microbeams subjected to different end conditions. Xiang-Yu Zhang et al. [17] studied the mechanical behavior of additively manufactured FGPMs used in biomedical applications. Y.H Dang et al. [18] also discussed free vibration characteristics due to porosities happening inside FGM samples of the graphene reinforced porous nanocomposite cylindrical shell with a spinning motion. Tran Van Lien et al. [19] conducted free vibration analysis of the functionally graded plates resting on various elastic foundations using a mathematical formulation based on a simple quasi-3D theory with both Reddy and the new trigonometric shear functions. Saidi and Sahla [20] employed vibration analysis of functionally graded plates with porosity composed of a mixture of Aluminium (Al) and Alumina ( $Al_2O_3$ ) embedded in an elastic medium. Vyacheslav and Tomasz [21] provided three-dimensional modeling of free vibrations and static response of functionally graded material (FGM) sandwich plates. A.F. Mota et al. [22] studied the dynamic response of porous functionally graded nanocomposite plates, using different porosity distributions. Yantao Zhang [23] investigated the influences of material porosity and volume fraction on the free damped vibration characteristics of functionally graded sandwich plates with porosities based on classical boundary conditions. Many researchers have used classical plate theory (CPT) to construct a mathematical model of sandwich structures for static and dynamic problems [24,25]. Recently, however, the FGPMs have found new and essential applications in the investigation of FGM structures, which today is a topical field of research.

From the above review of the literature, it is found that most researchers are interested in studying the free vibration analysis of FGM sandwich plates, but limited research work is available that takes into account the porous metal properties for both face sheets and core material in their analysis.

In the present study, the free vibration characteristics of the functionally graded sandwich plate with uniform distribution of porosities varying smoothly through the core thickness direction are investigated. A new approximate analytical solution (Rayleigh-Ritz method) including porous stiffness coefficients is developed based on classical plate constitutive equations. The material properties of FGM core layers are assumed to vary smoothly and continuously through the direction of thickness only. Various parameters which influence free vibration are considered, such as the porous factor, gradient index, plate geometrical ratios, and boundary conditions. The numerical results are carried out and compared with the approximated solution to validate the

accuracy of this modification. As such, the paper reports on a comprehensive study of porous FGM materials and provides useful analysis and results for the use of such materials in the engineering industry.

The paper is organized as follows. The next section will include an introduction to the free vibration of thin FG plates and a brief overview of the classical plate theory, describing the approximated Ryleigh-Ritz method used in the present work, and finite element analysis. Section 3 gives the convergence and verification study as well as frequent results covering the effects of the various parameters of the FG core on the free vibration characteristics of functionally graded sandwich plates. Finally, several key conclusions and useful proposals for further research on these structures are presented in the last section.

## 2. Problem formulation

### 2.1. Constitutive equations

This section includes analytical solution procedures for treating vibration problems related to FG plates with porous metal. An FGM plate made of ceramic–metal is employed in this study. The plate's length, width, and thickness are denoted by  $a$ ,  $b$  and  $h$ , respectively. The top surface's material structure ( $z = h/2$ ) is assumed to be ceramic-rich, and it constantly varies from the bottom surface's metal-rich surface ( $z = -h/2$ ). On the middle surface of the plate, a cartesian coordinate system ( $x, y, z$ ) is adopted to describe the plate motion, where in-plane coordinates are represented by  $x$  and  $y$ , while the  $z$  denotes the out-of-plane coordinate of the plate and the origin is at one of the plate corners. Most of the literature finds that the influences of Poisson's ratio are ignored, so it is assumed to be unchanged in this investigation. Assuming the classical or Kirchhoff's plate theory (CPT) given on the FG plate, the displacement field is assumed as [26],

$$\begin{aligned} u_x(x, y, z) &= -z \frac{\partial w}{\partial x} \\ u_y(x, y, z) &= -z \frac{\partial w}{\partial y} \\ u_z(x, y, z) &= w(x, y) \end{aligned} \quad (1)$$

where  $u_x, u_y$ , and  $u_z$  represented the displacement parameters through the line of coordinates of a certain point on the  $x$ - $y$  plane, and  $w$  is the transverse deflection of a point on the mid-plane ( $x$ - $y$  plane). Transverse shear deformation is neglected in Kirchhoff's case; on that is, deformation is due to bending and in-plane stretching. The stress-strain relations are given by [27],

$$\begin{pmatrix} \varepsilon_{xx} \\ \varepsilon_{yy} \\ \gamma_{xy} \end{pmatrix} = \begin{pmatrix} \frac{\partial u_x}{\partial x} \\ \frac{\partial u_y}{\partial y} \\ \frac{\partial u_x}{\partial y} + \frac{\partial u_y}{\partial x} \end{pmatrix} = \begin{pmatrix} -z \frac{\partial^2 w}{\partial x^2} \\ -z \frac{\partial^2 w}{\partial y^2} \\ -2z \frac{\partial^2 w}{\partial x \partial y} \end{pmatrix} \quad (2)$$

In Eq. 2, the normal strains in terms in  $x$  and  $y$  directions are  $\varepsilon_{xx}$  and  $\varepsilon_{yy}$ , while  $\gamma_{xy}$  indicates to shear strain component. According to Hooke's law, the following matrix form can be used to describe the relationships of the stress and strain expressions at a given point of the functionally graded plate,

$$\begin{pmatrix} \sigma_{xx} \\ \sigma_{yy} \\ \tau_{xy} \end{pmatrix} = \begin{pmatrix} A_{11} & A_{12} & 0 \\ A_{21} & A_{22} & 0 \\ 0 & 0 & A_{66} \end{pmatrix} \begin{pmatrix} \varepsilon_{xx} \\ \varepsilon_{yy} \\ \gamma_{xy} \end{pmatrix} \quad (3)$$

The components of the normal and shear stress  $\sigma_{xx}$ ,  $\sigma_{yy}$  and  $\tau_{xy}$  can be used to construct the reduced stiffness parameters  $A_{ij}$  ( $i, j = 1, 2, 6$ ),

$$\begin{aligned} A_{11} &= A_{22} = \frac{E(z)}{1-\nu^2} \\ A_{12} &= A_{21} = \frac{\nu E(z)}{1-\nu^2} \\ A_{66} &= \frac{E(z)}{2(1+\nu)} \end{aligned} \quad (4)$$

The materials properties  $E, \nu$  represent Young's modulus and Poisson's ratio of the functionally graded plate. The linear constitutive relations of an FG plate, such as the bending and twisting moments  $M_{xx}, M_{yy}$  and  $M_{xy}$  respectively on a plate element. The pure bending case can be written as, [23,28],

$$\begin{pmatrix} M_{xx} \\ M_{yy} \\ M_{xy} \end{pmatrix} = \int_{-h/2}^{h/2} \begin{pmatrix} \sigma_x \\ \sigma_y \\ \tau_{xy} \end{pmatrix} z \, dz \quad (5)$$

### 2.2. Energy expressions model

The strain energy  $U$  stored in an elastic body, for a general state of stress, is given by,

$$U = \frac{1}{2} \iiint_V \left( \sigma_x \varepsilon_x + \sigma_y \varepsilon_y + \sigma_z \varepsilon_z + \tau_{xy} \gamma_{xy} + \tau_{xz} \gamma_{xz} + \tau_{yz} \gamma_{yz} \right) dx dy dz \quad (6)$$

Integration extends over the entire body volume for thin plates  $\sigma_z, \gamma_{xz}, \gamma_{yz}$  can be omitted. Thus, introducing Hooke's law, the above expression is reduced to the following form involving only stresses and elastic constants,

$$U = \iiint_V \left( \frac{1}{2E} (\sigma_x^2 + \sigma_y^2 - 2\nu \sigma_x \sigma_y) + \frac{1}{2G} \tau_{xy}^2 \right) dx dy dz \quad (7)$$

$$U = \frac{1}{2} \int_{\Omega} \left( \int_{-h/2}^{h/2} (\sigma_{xx} \varepsilon_{xx} + \sigma_{yy} \varepsilon_{yy} + \tau_{xy} \gamma_{xy}) dz \right) dx dy \quad (8)$$

The kinetic energy (T) of the plate in cartesian coordinates at any instant can be expressed as,

$$T = \frac{1}{2} \int_{\Omega} \left( \int_{-h/2}^{h/2} \rho(z) \left( \frac{\partial u_z}{\partial t} \right)^2 dz \right) dx dy \quad (9)$$

where  $\Omega$  denotes the mid-plane (domain) of the FG plate. Using Eqs. (1), (2), and (3) in Eqs. (8) and (9) lead to the total potential energy function U,

$$U = \frac{1}{2} \int_{\Omega} \left( D_{11} \left( \left( \frac{\partial^2 w}{\partial x^2} \right)^2 + \left( \frac{\partial^2 w}{\partial y^2} \right)^2 \right) + 2D_{12} \frac{\partial^2 w}{\partial x^2} \frac{\partial^2 w}{\partial y^2} + 4D_{66} \left( \frac{\partial^2 w}{\partial x \partial y} \right)^2 \right) dx dy \quad (10)$$

$$T = \frac{1}{2} \int_{\Omega} I_0 \left( \frac{\partial w}{\partial t} \right)^2 dx dy \quad (11)$$

where, the flexural rigidity coefficients  $D_{11}$ ,  $D_{12}$ ,  $D_{66}$  in Eq. 10 can be evaluated as,

$$(D_{11}, D_{12}, D_{66}) = \int_{-h/2}^{h/2} (A_{11}, A_{12}, A_{66}) z^2 dz \quad (12)$$

### 2.3. Functionally graded sandwich plates with porosity

The continuous variation of material properties of FG plate constituents can be represented by an exponential law, a sigmoid law, and a power-law variation. In the present study, the FG plate is assumed to follow power-law variation. The ceramic volume fraction  $V_c$  can be defined as [29],

$$V_c(z) = \left( \frac{z+h/2}{h} \right)^k \quad (13)$$

The volume fraction sum of metal and ceramic is stated as,  $V_m(z) + V_c(z) = 1$ , where  $V_m$  is the volume fractions of metal,  $k$  is the power-law variation index and is a non-negative variable parameter, in which  $k \in [0, \infty)$ . The value of  $k=0$  represents a fully ceramic plate, whereas  $k=\infty$  indicates a fully metallic plate. The material property of the FGM plate is supposed to change continually along the thickness direction and obey power-law distribution in the following,

$$P(z) = P_m + (P_c - P_m) \left( \frac{2z+h}{2h} \right)^k \quad (14)$$

In Eq. (15),  $P_m$  and  $P_c$  are the values of material properties of ceramic and metal, constituents of the FG plate, respectively. For our present formulations, the material properties, viz. Young's modulus ( $E$ ) and mass density ( $\rho$ ) are taken to vary throughout the gradient direction except for Poisson's ratio ( $\nu$ ) remains constant. The material properties of an FGM plate with porosity are assumed to vary

continuously within the plate thickness according to the power-law distribution ( $k$ ), ( $\beta$ ) is the porosity distribution factor based on plate thickness. For the even distribution of porosities inside the material, the general Young's modulus  $E(z)$  and mass density  $\rho(z)$  of the imperfect FGM plate can be written, respectively, as [30],

$$E(z) = (E_c - E_m) \left( \frac{2z+h}{2h} \right)^k + E_m - (E_c + E_m) \frac{\beta}{2} \quad (15)$$

$$\rho(z) = (\rho_c - \rho_m) \left( \frac{2z+h}{2h} \right)^k + \rho_m - (\rho_c + \rho_m) \frac{\beta}{2} \quad (16)$$

Consider a rectangular plate of length  $a$  and width  $b$  with its four edges simply supported, as shown in Figure 1. Assume the mechanical properties  $E_1 = E_2 = E$ ,  $\nu_1 = \nu_2 = \nu$  and the mass density  $\rho_1 = \rho_2 = \rho$ ; and the thickness of two face sheets is the same (i.e.,  $h_1 = h_2$ ), then the general representation of the flexural rigidity and inertia for the sandwich plate ( $D_{ij}$  &  $I_0$ ) can be written as

$$D_{11} = \left( \begin{aligned} & \int_{-(\frac{h+h_1}{2})}^{-\frac{h}{2}} \left( \frac{z^2}{(1-\nu^2)} E(z) \right) dz + \\ & \frac{1}{(1-\nu^2)} \left( \int_{-\frac{h}{2}}^{\frac{h}{2}} \left( (E_c - E_m) \left( \frac{z}{h} + \frac{1}{2} \right)^k - (E_c + E_m) \frac{\beta}{2} + E_m \right) z^2 dz \right) \\ & + \int_{\frac{h}{2}}^{\frac{h+h_2}{2}} \left( \frac{z^2}{(1-\nu^2)} E(z) \right) dz \end{aligned} \right) \quad (17)$$

$$D_{11} = \left( \begin{aligned} & \frac{(E_c - E_m) h^3}{(1-\nu^2)} \left( \frac{1}{k+3} - \frac{1}{k+2} + \frac{1}{4(k+1)} \right) \\ & + \frac{E_m h^3}{12(1-\nu^2)} - \frac{(E_c + E_m) \beta h^3}{24(1-\nu^2)} \\ & + \frac{EUP}{12(1-\nu^2)} \{ (h + 2h_1)^3 - h^3 \} \end{aligned} \right) \quad (18)$$

$$D_{12} = \int_{-h/2}^{h/2} A_{12} z^2 dz = \int_{-h/2}^{h/2} \frac{\nu E(z)}{1-\nu^2} z^2 dz \quad (19)$$

$$D_{12} = \left( \begin{aligned} & \frac{\nu(E_c - E_m) h^3}{(1-\nu^2)} \left( \frac{1}{k+3} - \frac{1}{k+2} + \frac{1}{4(k+1)} \right) + \frac{E_m h^3}{12(1-\nu^2)} \\ & - \frac{(E_c + E_m) \beta h^3}{24(1-\nu^2)} + \frac{\nu E}{(1-\nu^2)} \left( \frac{2 \left( \frac{h}{2} + h_1 \right)^3}{3} - \frac{h^3}{12} \right) \end{aligned} \right) \quad (20)$$

$$D_{66} = \int_{-h/2}^{h/2} A_{66} z^2 dz = \int_{-h/2}^{h/2} \frac{E(z)}{2(1+\nu)} z^2 dz \quad (21)$$

$$D_{66} = \left( \begin{aligned} & \frac{(E_c - E_m) h^3}{2(1+\nu)} \left( \frac{1}{k+3} - \frac{1}{k+2} + \frac{1}{4(k+1)} \right) + \frac{E_m h^3}{24(1+\nu)} - \\ & \frac{(E_c + E_m) \beta h^3}{48(1+\nu)} + \frac{24E}{(1+\nu)} \left( 8 \left( \frac{h}{2} + h_1 \right)^3 - h^3 \right) \end{aligned} \right) \quad (22)$$

and,

$$I_0 = \int_{-\frac{h}{2}}^{\frac{h}{2}} \rho(z) dz \tag{23}$$

where  $I_0$  is the total moment of inertia of the FGM sandwich plate which can be expressed in term of the porosities and gradient index as,

$$I_0 = \frac{(\rho_c - \rho_m)h}{(k+1)} + \rho_m h - (\rho_c + \rho_m) \frac{\beta h}{2} + 2\rho h_1 \tag{24}$$

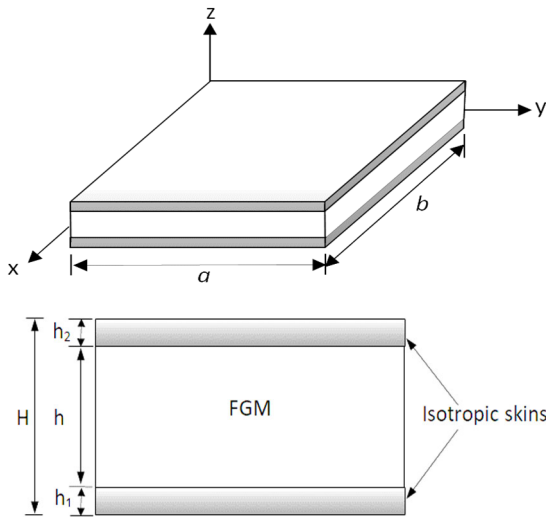


Fig. 1. Sandwich plate with FGM core and isotropic skins

To evaluate the behaviour of the deflection plate as a function of  $x$  and  $y$  directions that satisfy the boundary conditions. The assumed harmonic type function of the displacement component can be expressed as [10,31],

$$w(x, y, t) = W(x, y) \cos \omega t \tag{25}$$

$W(x, y)$  and  $\omega$  are the respective maximum deflection and natural frequency of free vibration. Now, by using Eq. (25) in Eqs. (10), and (11), the maximum strain energy ( $U_{max}$ ) and kinetic energy ( $T_{max}$ ), can be obtained as follows,

$$U_{max} = \frac{1}{2} \int_{\Omega} \left( D_{11} \left( \left( \frac{\partial^2 W}{\partial x^2} \right)^2 + \left( \frac{\partial^2 W}{\partial y^2} \right)^2 \right) + 2D_{12} \frac{\partial^2 W}{\partial x^2} \frac{\partial^2 W}{\partial y^2} + 4D_{66} \left( \frac{\partial^2 W}{\partial x \partial y} \right)^2 \right) dx dy \tag{26}$$

or, alternately

$$U_{max} = \int_{\Omega} D_{11} \left( \left( \frac{\partial^2 W}{\partial x^2} \right)^2 + \left( \frac{\partial^2 W}{\partial y^2} \right)^2 + 2\nu \frac{\partial^2 W}{\partial x^2} \frac{\partial^2 W}{\partial y^2} + 2(1-\nu) \left( \frac{\partial^2 W}{\partial x \partial y} \right)^2 \right) dx dy \tag{27}$$

$$T_{max} = \frac{\omega^2}{2} \int_{\Omega} I_0 W^2 dx dy \tag{28}$$

To find  $n$  natural frequencies using the Rayleigh-Ritz method, the deflection function  $W(x, y)$  can be used as follows [32,33],

$$W(x, y) = \sum_{i=1}^n C_i \phi_i(x, y) \tag{29}$$

where  $C_i$ , are  $n$  unknown constant and  $\phi_i(x, y)$  are  $n$  known arbitrary (assumed) functions of  $(x, y)$ , and  $W(x, y)$  satisfies the geometric edge conditions and can be expressed as,

$$\phi_i(x, y) = \Pi \psi_i(x, y), i = 0, 1, 2, \dots, n \tag{30}$$

Here,  $n$  is the number of polynomials included in the deflection shape function. The function  $\Pi = x^{a_1} y^{a_2} (a - x)^{a_3} (b - y)^{a_4}$  with the exponents  $a_1, a_2, a_3,$  and  $a_4$ , governing the different geometric BCs. The parameter  $a_1=0, 1$  or  $2$  according to as the edge  $x=0$  is free, simply supported or clamped. Same interpretations can be used to the parameters  $a_2, a_3,$  and  $a_4$  corresponding to the sides  $y=0, x=a,$  and  $y=b,$  respectively. Moreover, expansion coefficients of the binomial  $\psi_i$  will be obtained from the triangular arrangement available in Pascal's triangle as given in Table 1.

Table 1.

Values of expansion coefficients  $\psi_i$

i	1	2	3	4	5	6	7	8	9	10
$\psi_i$	1	x	y	$x^2$	xy	$y^2$	$x^3$	$x^2y$	$xy^2$	$y^3$

Now, taking the partial derivative of  $\omega^2$  with respect to unknown constants as,  $\partial \omega^2 / \partial C_i = 0, i = 1, 2, 3, \dots, n$ . Thus, Eq. (27) can be further simplified to become similar to the free vibration eigenvalue problem,

$$([K]_{n \times n} - \lambda^2 [M]_{n \times n}) \{\delta\} = 0 \tag{31}$$

where  $[K]_{n \times n}$  represents the stiffness coefficients matrix while  $[M]_{n \times n}$  is the inertia coefficients matrix of the functionally graded sandwich plate, and  $\{\delta\}$  is the column vector of unknown constant coefficients. Solutions of the standard generalized eigenvalue problem, the frequencies and mode shapes of the FG porous sandwich plate are obtained from Eq. (31). By equating  $U_{max}$  and  $T_{max}$ , the Rayleigh quotient ( $\omega^2$ ) can be expressed as,

$$\omega^2 = \frac{U_{max}}{\int_{\Omega} I_0 W^2 dx dy} \tag{32}$$

$$\omega^2 = \frac{\int_{\Omega} D_{11} \left( \left( \frac{\partial^2 W}{\partial x^2} \right)^2 + \left( \frac{\partial^2 W}{\partial y^2} \right)^2 + 2\nu \frac{\partial^2 W}{\partial x^2} \frac{\partial^2 W}{\partial y^2} + 2(1-\nu) \left( \frac{\partial^2 W}{\partial x \partial y} \right)^2 \right) dx dy}{\int_{\Omega} I_0 W^2 dx dy} \tag{33}$$

The non-dimensional frequency parameters of the functionally graded sandwich plate may be obtained as,

$$\psi = \frac{\omega L^2}{H} \sqrt{\frac{\int_{-h/2}^{h/2} \rho(z) dz}{\int_{-h/2}^{h/2} E(z) dz}} \quad (34)$$

where, ( $H$ ) is the sandwich plate's total height, to solve the above equations, a code written using MATLAB software is used. The FG core considered here consists of Alumina and Aluminium and the skins are made of structural steel with the material properties listed in Table 2.

Table 2. Material properties employed in the FG sandwich plates

Property	FG core		Skins (Steel)
	Aluminium (Al)	Ceramic (Al <sub>2</sub> O <sub>3</sub> )	
Modula's of Elasticity, GPa	70	380	210
Mass density, Kg/m <sup>3</sup>	2702	3800	7800
Poisson's ratio	0.3	0.3	0.3

### 2.4. Numerical investigation

FEA allows the analysis of various structures without improving and including complex relations. Hence, it is important to evaluate most design problems [34-42]. In this work, a numerical investigation was carried out to evaluate the free vibration characteristics of FGM sandwich plates with porous metal. As a consequence, numerical simulation is used to develop the performance, stability, and vibration responses of the generated models and to check the accuracy of the current study. The commercial finite element code ANSYS program 2020 R2 is used to simulate the free vibration of the sandwich plate [39, 43-50]. A 3D model of an FG sandwich plate is built and the boundary conditions for each side of the structure are applied as shown in Figure 2. A mesh convergence study was carried out and the precision mesh size was selected. Then, the model was meshed with an 8-node SOLID186 element type for both the face sheets and the core with a total number of elements of 40000, as shown in Figure 3. At the connection area of the layers and amongst the layers and skins of the sandwich, all parts are assumed to be perfectly bonded together [51-60]. The skin parts are considered isotropic materials with properties shown in Table 2. Furthermore, the mechanical properties of the porous metal core are calculated using equations 14, 15, and 16 by building a separate program in Microsoft Excel 2019.

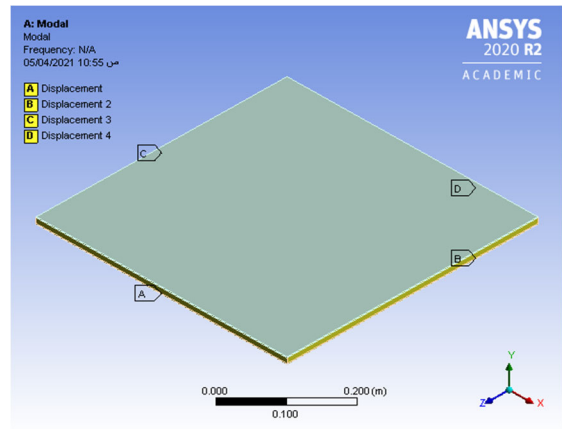


Fig. 2. FGM Sandwich plate

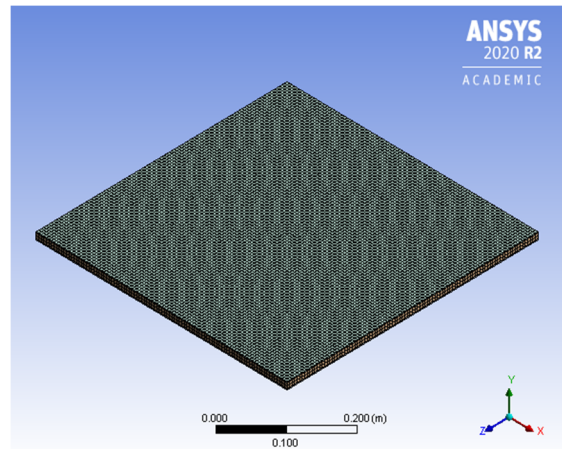


Fig. 3. Meshed model

Table 3. Material properties of the porous metal core calculated using Eqs. (15-17)

Porosity, $\beta$	Power-law index, $k$	E, GPa	$\rho$ , kg/m <sup>3</sup>	$\nu$
0.0	0.5	281.7	3451.9	0.3
0.0	1.0	225.0	3251.0	0.3
0.0	5.0	106.9	2832.8	0.3
0.1	0.5	257.0	3126.8	0.3
0.1	1.0	200.3	2925.9	0.3
0.1	5.0	82.20	2507.7	0.3
0.2	0.5	232.2	2801.7	0.3
0.2	1.0	175.5	2600.8	0.3
0.2	5.0	57.40	2182.6	0.3
0.3	0.5	207.5	2476.6	0.3
0.3	1.0	150.8	2275.7	0.3
0.3	5.0	32.70	1857.5	0.3

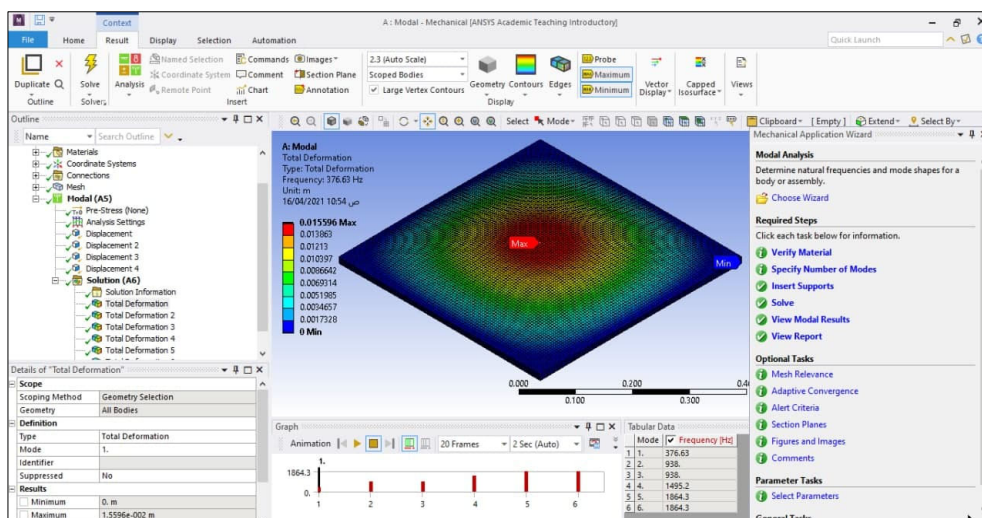


Fig. 4. View of Modal Analysis of FGM sandwich plate

The sample of results of the FG core properties at porosity ( $\beta = 0$  to 0.3) and power-law index ( $k=0.5, 1$ , and 5) is presented in Table 3. Modal analysis is, along with linear static analysis, one of the two most common types of FE analysis. The modal analysis is carried out to generate substep results of the free vibration characteristics (natural frequencies and the mode shapes) for the selected FG models based on various parameters previously discussed as shown in Figure 4.

### 3. Results and discussion

The free vibration analysis of an FGM sandwich plate with porous metal using the Rayleigh-Ritz method is presented in this study. The FG core materials are assumed to be distributed to the upper and lower plate parts. Numerical validation is performed using ANSYS 2020 R2 to prove the accuracy and performance of the proposed solution.

This section investigates a number of numerical examples concerning the non-dimensional fundamental frequency and mode shapes of the sandwich plate with different boundary conditions integrated with porosity factors  $\beta$  and gradient indices  $k$ .

The FGM core is made of aluminium and ceramic ( $Al/Al_2O_3$ ) with different heights ( $h=10, 15, 20, 1.5$ , and 25 mm), while the facings are made of steel alloy with varying thicknesses ( $h_f=0.5, 1.5.2$ , and 2.5 mm).

Plates have the following dimensions: ( $a=b=0.5$  m). In order to present the numerical results in tabular and

graphical form, the following non-dimensional frequency parameters are used:

$$\psi = \frac{\omega L^2}{h} \sqrt{\frac{\rho_0}{E_0}} \quad (35)$$

where,  $\omega$  is the natural frequency,  $\rho_0=1$  Kg/m<sup>3</sup> and  $E_0=1$  GPa [3].

Table 4 gives analytical and numerical results of the frequency parameter for sandwich FGM plate at four different slenderness ratios, ( $a/H= 10, 20, 30$ , and 100) porous factor ( $\beta=0,0.1,0.2$  and 0.3), and gradient index ( $k=0, 0.5, 1, 2$ , and 5), respectively. It is found that the natural frequencies increase when the porous parameter increasing and decrease with increasing gradient index due to the decrease in the material rigidity. Also, it is clear from table 4 that for a thin plate, the suggested approximated analytical solution by Rayleigh-Ritz is close to the FEA solutions. When the plate thickness increases, the error percentage in CPT will be higher, for example, there is an apparent error between the analytical and numerical solution reach to 13% at slenderness ratio ( $a/H=10$ ), and this percentage is affected by power-law index and porous factor for same FG plate thickness.

In Table 5, the numerical results for the first six total deformation frequencies of FG square sandwich plates at porosity ( $\beta = 0$  to 0.3), slenderness ratio ( $a/H = 20$ ), and gradient index ( $k = 1$ ) are considered. From the results obtained, it is evident that the present results indicate that the natural frequency increases with porosity, and for higher modes of the natural frequency there are not any big changes modes of the natural frequency there are not any big

changes. This is due to the high stability of the sandwich plate at large deformations.

Convergence of the nondimensional frequency of FGM sandwich plate with porous core and steel face sheet (2 mm), under the effect of five types of BCs, is presented in Table 6 with respect to thickness ratio ( $a/H = 50$ ) and various porosity factors. The influence of the porous factor and the

gradient index has also been investigated. It is discovered that the value of the frequency parameter increases as the number of constraints in the selected model increases; for example, at porous factor ( $\beta = 0.1$ ) and with a gradient index ( $k = 1$ ), the frequency parameter in the CCCC model is (2.348), while for CCCS it was (2.114), SCSC was equal (2.085), and SSSC was equal (1.998).

Table 4.

Analytical and numerical results of the first nondimensional frequencies of (Al/Al<sub>2</sub>O<sub>3</sub>) square plate for various parameters

$a/H$	Porosity, $\beta$	Power-law index, $k$									
		0		0.5		1		2		5	
		Ana.	Num.	Ana.	Num.	Ana.	Num.	Ana.	Num.	Ana.	Num.
10	0	1.855	1.783	1.642	1.639	1.580	1.529	1.536	1.399	1.458	1.275
	0.1	1.875	1.819	1.663	1.648	1.585	1.533	1.545	1.429	1.445	1.287
	0.2	1.892	1.836	1.681	1.662	1.586	1.542	1.552	1.436	1.437	1.295
	0.5	2.009	1.929	1.734	1.719	1.616	1.649	1.565	1.521	1.369	1.316
20	0	1.862	1.838	1.685	1.700	1.634	1.612	1.587	1.502	1.527	1.365
	0.1	1.879	1.860	1.694	1.709	1.642	1.617	1.590	1.498	1.534	1.374
	0.2	1.891	1.879	1.711	1.726	1.654	1.623	1.593	1.494	1.540	1.386
	0.5	1.981	1.965	1.758	1.777	1.680	1.648	1.607	1.470	1.559	1.594
50	0	1.942	1.931	1.837	1.853	1.807	1.794	1.777	1.731	1.759	1.722
	0.1	1.964	1.958	1.851	1.869	1.816	1.806	1.788	1.740	1.765	1.729
	0.2	1.979	1.977	1.864	1.881	1.839	1.819	1.801	1.780	1.773	1.748
	0.5	2.065	2.048	1.919	1.941	1.883	1.868	1.850	1.839	1.812	1.792
100	0	2.209	2.215	2.195	2.189	2.145	2.128	2.134	2.119	2.118	2.108
	0.1	2.232	2.229	2.169	2.172	2.157	2.160	2.146	2.151	2.135	2.124
	0.2	2.242	2.236	2.188	2.179	2.176	2.170	2.165	2.148	2.157	2.137
	0.5	2.314	2.294	2.255	2.265	2.240	2.228	2.231	2.219	2.221	2.198

Table 5.

Total deformation frequencies (Hz) for FG square sandwich plates ( $a/H = 20, k = 1$ )

Porosity	Total Deformation					
	Frequency 1	Frequency 2	Frequency 3	Frequency 4	Frequency 5	Frequency 6
0.00	681.05	1680.70	1680.70	2656.11	3293.52	3293.52
0.03	681.08	1680.75	1680.75	2655.83	3293.02	3293.03
0.07	681.21	1680.99	1681.00	2655.84	3292.88	3292.90
0.10	681.42	1681.43	1681.43	2656.16	3293.09	3293.11
0.13	681.73	1682.06	1682.06	2656.77	3293.63	3293.66
0.17	682.13	1682.87	1682.88	2657.66	3294.50	3294.53
0.20	682.62	1683.87	1683.88	2658.83	3295.68	3295.71
0.23	683.20	1685.06	1685.06	2660.25	3297.13	3297.17
0.27	683.87	1686.41	1686.42	2661.91	3298.85	3298.89
0.30	684.63	1687.94	1687.95	2663.80	3300.79	3300.83

Table 6.

Frequency Parameter of (Al/Al<sub>2</sub>O<sub>3</sub>) square sandwich plate with various porosity factors for different boundary conditions

BCs	$a/H$	Face sheet thickness, mm	Power-law index, $k$	Porosity factor, $\beta$			
CCCC	50	2	0	2.58	2.60	2.62	2.64
			0.5	2.43	2.45	2.46	2.48
			1	2.34	2.35	2.35	2.41
			2	2.23	2.23	2.23	2.25
			5	2.09	2.09	2.11	2.12
			0	2.32	2.33	2.34	2.35
CCCS	50	2	0.5	2.19	2.20	2.21	2.22
			1	2.11	2.11	2.12	2.13
			2	2.01	2.01	2.02	2.08
			5	1.88	1.88	1.90	1.91
			0	2.18	2.19	2.22	2.23
			0.5	2.07	2.08	2.10	2.11
SSSC	50	2	1	1.99	2.00	2.02	2.03
			2	1.90	1.91	1.91	1.92
			5	1.80	1.82	1.83	1.84
			0	1.94	1.95	1.97	1.99
			0.5	1.85	1.86	1.88	1.90
			1	1.79	1.81	1.82	1.83
SSSS	50	2	2	1.73	1.74	1.75	1.76
			5	2.57	2.591	2.61	2.63
			0	2.35	2.36	2.37	2.41
			0.5	2.23	2.23	2.25	2.26
			1	2.09	2.09	2.11	2.12
			2	2.04	2.08	2.11	2.14
CSCS	50	2	5	1.07	1.07	2.14	2.16

However, it is also concluded that when the gradient index increases, the overall stiffness of the plate decreases, and affects the frequency parameter's value. Graphical representations of the natural frequency relationships for simply supported FG sandwich plates given are shown in Figures 5-8. Figure 5 shows a 3D surface for the fundamental frequency at porosity ( $\beta = 0$ ), with a face sheet thickness of 2 mm, for various FGM thicknesses. In a similar fashion, Figure 6 shows the same representation of porosity ( $\beta = 0.3$ ). Figures 7 and 8 present the fundamental frequency of a simply supported functionally graded sandwich plate by changing the gradient index from ( $k=0$ ) to ( $k=2$ ).

Based on the findings, it is concluded that the porosity coefficients play a crucial part in determining the stability of the FGM plate. As shown in Figure 9, one can plot the

variation of the frequency parameter of the rectangular sandwich plate with respect to aspect ratios. It is observed that the frequency parameter increases as the aspect ratio increases and that there is distinct convergence at lower aspect ratio values. It may also be viewed that frequency parameters are increasing with an increase in aspect ratios. This is due to the that the stiffness of the FG rectangular sandwich plate increases gradually with an increase in aspect ratios. Figure 10 shows the influence of the number of layers on the frequency parameter of the rectangular plate at three values of side to length ratios ( $a/b = 0.5, 1$  and  $2$ ) at gradient index ( $k=0.5$ ) and porosity ( $\beta = 0$ ). The figure shows that the stability of sandwich structure made of porous metal becomes more with an increase of the number of FG core layers for the same FGM thickness.

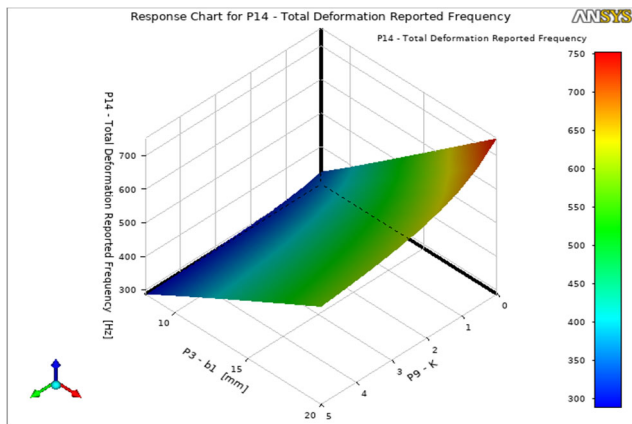


Fig. 5. 3D Surface for the fundamental frequency at  $(\beta=0)$ , for various FGM thickness

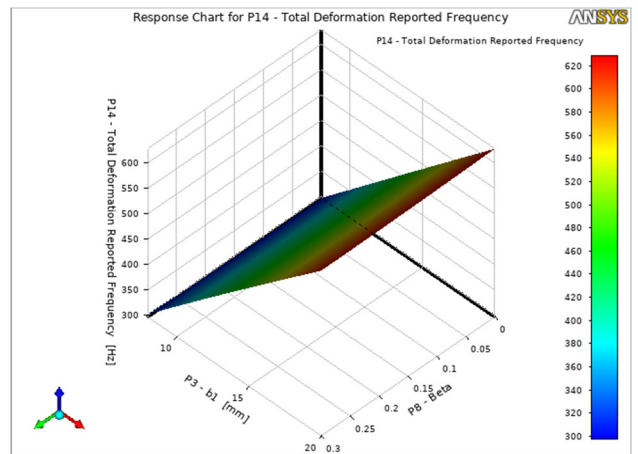


Fig. 8. 3D Surface for the fundamental frequency at gradient index  $(k=2)$ , for various FGM thickness

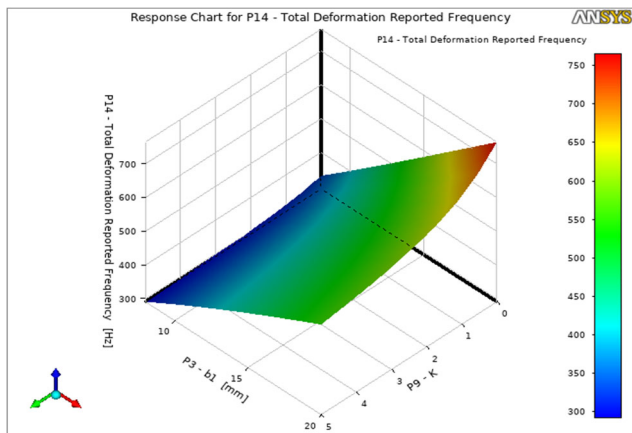


Fig. 6. 3D Surface for the fundamental frequency at  $(\beta=0.3)$ , for various FGM thickness

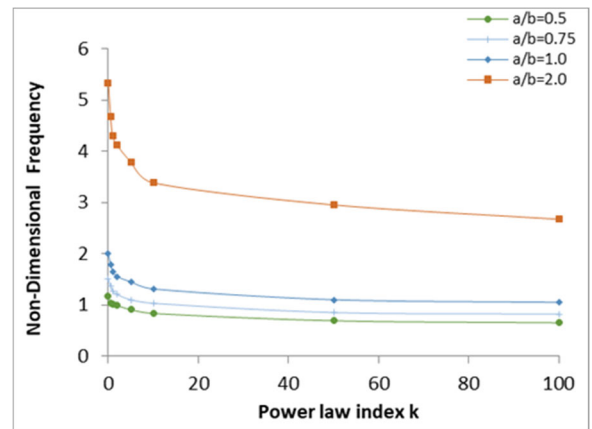


Fig. 9. Numerical results of the frequency parameter of a rectangular plate with different aspect ratios

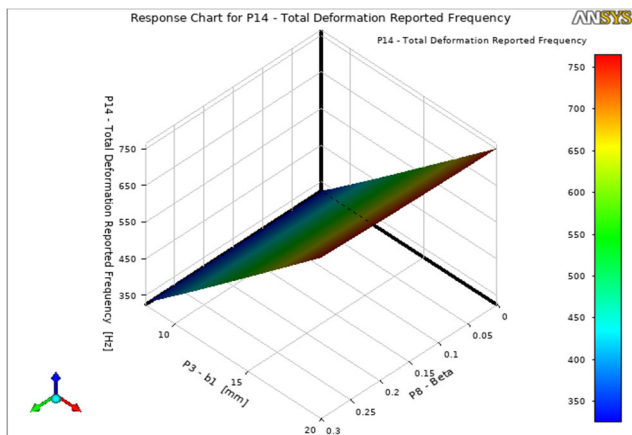


Fig. 7. 3D Surface for the fundamental frequency at gradient index  $(k=0)$ , for various FGM thickness

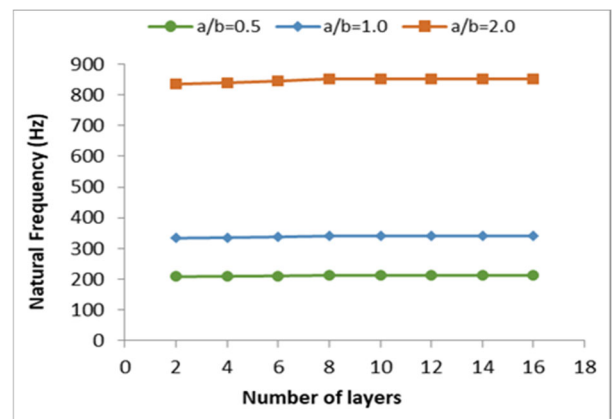


Fig. 10. Numerical results of the frequency for a different number of layers of FGM rectangular plate at  $(k=0.5)$

By non-dimensionalizing the circular frequency, the curves shown in Figures 11 and 12 state a 3 D surface for analytical results of the frequency parameter using MATLAB code results at porosity ( $\beta = 0$ , and  $\beta = 0.3$ ) respectively. It is clear that the frequency parameter increases with the increase in porosity due to an increase in the stiffness of the plate. Accordingly, in Figure 13, the first six deflections of 3-D numerical mode shapes are generated for a simply supported FG square sandwich plate at ( $\beta = 0$  and  $k=0.5$ ). Where the first mode shape is the bending mode, the lateral second and third are similar and the fourth one represents the torsional mode, while the fifth and sixth modes have the same results, but with a different configuration.

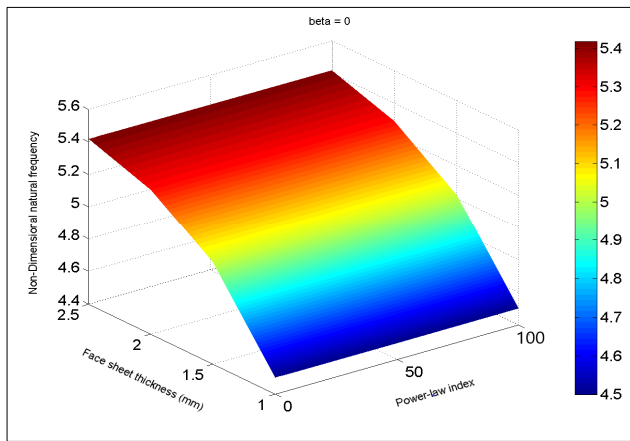


Fig. 11. Analytical results of the frequency parameter of the square sandwich plate at ( $\beta = 0$ )

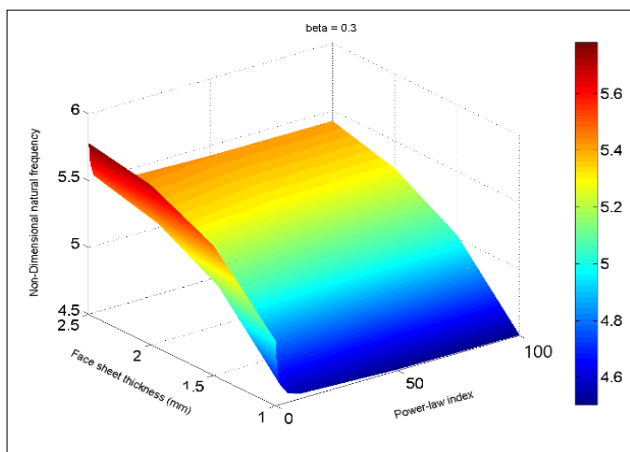


Fig. 12. Analytical results of the frequency parameter of the square sandwich plate at ( $\beta = 0.3$ )

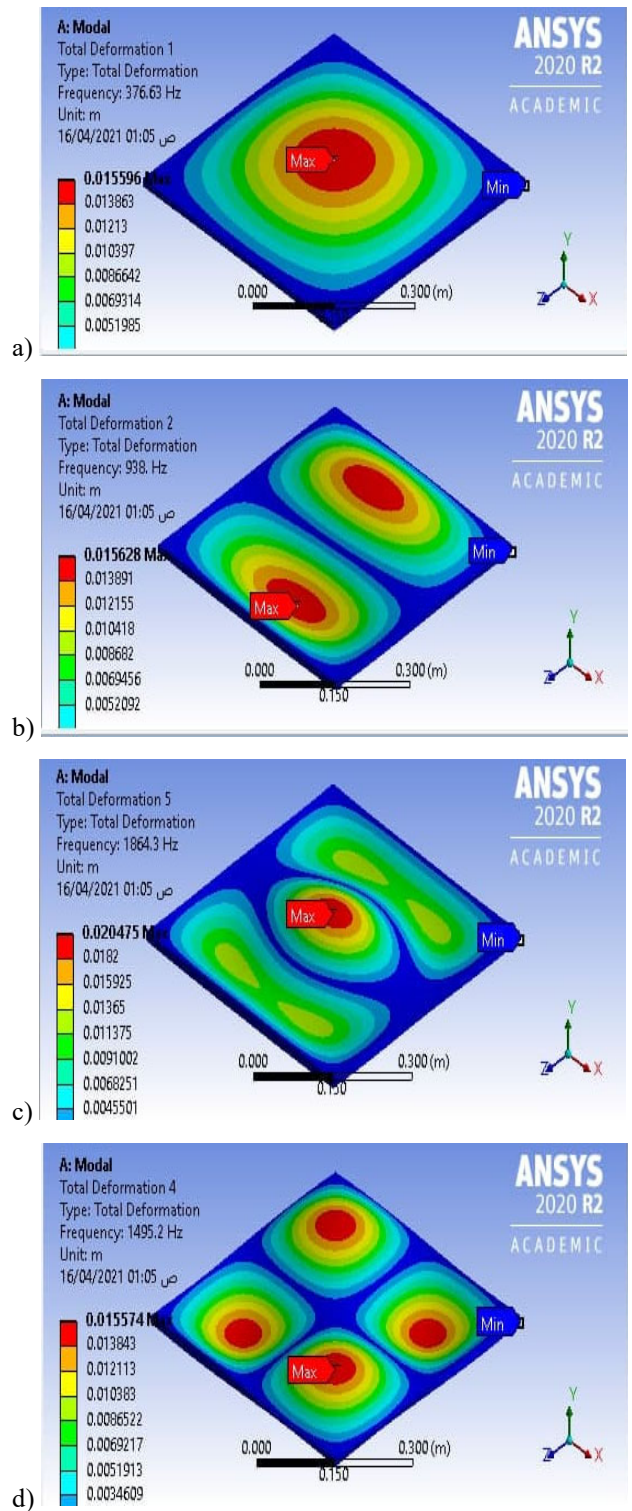


Fig. 13. The first four mode shapes for a square sandwich plate at ( $\beta = 0$ ,  $k = 0.5$ , and  $a/h=50$ ); a)-d) modes 1-4, respectively

## 4. Conclusions

The most commonly used FGM sandwich constructions are the FGM core with homogeneous skin. The contributions of the FG porous metal in the design of biomedical and aerospace structures can be considered for the features of lightweight and high bending stiffness by suitably selecting the core metal type and the number of layers. Free vibration analysis of functionally graded porous materials (FGPMs) with various edge conditions is considered in this work. The sandwich plate is made up of a two-phase porous metal (Ceramic-Aluminium) core that is glued to homogeneous steel plates on both sides with appropriate adhesion. The material properties, including the porosity volume fraction, are assumed to vary depending on the thickness of a power-law distribution.

A simple and accurate mathematical model is based on CPT principles and the Ryleigh-Ritz approximate technique was presented to identify natural frequencies of the FG sandwich plate based on various parameters. The numerical study using ANSYS Workbench 2020 R2 confirms the analytical solution results are carried out. The paper also investigates the effect of various parameters on the free vibration characteristics of FG sandwich plates, such as porous factor, gradient index, and aspect ratio. The following observations are based on the findings.

1. In both proposed methods of solution (analytical and numerical), natural frequency increases with increasing porous factor and decreases with increasing power-law index.
2. The Ryleigh-Ritz method is a very approximate and easy way to assess the free vibration analysis of an FGM sandwich structure, particularly when the model has a large number of parameters.
3. The graphs clearly show that as the power-law index increases, the values of natural frequency discrepancies drop significantly for all types of boundary conditions.
4. Numerical results show a remarkable convergence between the results obtained by the predicted proposed technique and those obtained numerically by the Ansys software, as the error percentage did not exceed 6%, indicating the reliability of the developed mathematical model in vibration analyses of functionally graded sandwich plates with porosities.

FGPMs offer a wide range of industrial applications. As a result, more research on the behaviour of such structures is required, including but not limited to optimization studies and the accomplishment of a full experimental program.

## References

- [1] E.K. Njim, M. Al-Waily, S.H. Bakhy, A Critical Review of Recent Research of Free Vibration and Stability of Functionally Graded Materials of Sandwich Plate, IOP Conference Series: Materials Science and Engineering 1094 (2021) 012081. DOI: <https://doi.org/10.1088/1757-899X/1094/1/012081>
- [2] A. Garg, M.O. Belarbi, H.D. Chalak, A. Chakrabarti, A review of the analysis of sandwich FGM structures, Composite Structures 258 (2021) 113427. DOI: <https://doi.org/10.1016/j.compstruct.2020.113427>
- [3] A. Menasria, A. Kaci, A.A. Bousahla, F. Bourada, A. Tounsi, K.H. Benrahou, A. Tounsi, E.A. Adda Bedia, S.R. Mahmoud, A four-unknown refined plate theory for dynamic analysis of FG-sandwich plates under various boundary conditions, Steel and Composite Structures 36/3 (2020) 355-367. DOI: <http://dx.doi.org/10.12989/scs.2020.36.3.355>
- [4] I. Katili, J.L. Batoz, I.J. Maknun, A.M. Katili, On static and free vibration analysis of FGM plates using an efficient quadrilateral finite element based on DSPM, Composite Structures 261 (2021) 113514. DOI: <https://doi.org/10.1016/j.compstruct.2020.113514>
- [5] J. Yang, H.S. Shen, Dynamic response of initially stressed functionally graded rectangular thin plates, Composite Structure 54/4 (2001) 497-508. DOI: [https://doi.org/10.1016/S0263-8223\(01\)00122-2](https://doi.org/10.1016/S0263-8223(01)00122-2)
- [6] P.V. Vinh, N.T. Dung, N.C. Tho, D.V. Thom, L.K. Hoa, Modified single variable shear deformation plate theory for free vibration analysis of rectangular FGM plates, Structures 29 (2021) 1435-1444. DOI: <https://doi.org/10.1016/j.istruc.2020.12.027>
- [7] A.M. Zenkour, A comprehensive analysis of functionally graded sandwich plates: Part 2 - Buckling and free vibration, International Journal of Solids and Structures 42/18-19 (2005) 5243-5258. DOI: <https://doi.org/10.1016/j.ijsolstr.2005.02.016>
- [8] J. Liu, C. Hao, W. Ye, F. Yang, G. Lin, Free vibration and transient dynamic response of functionally graded sandwich plates with power-law nonhomogeneity by the scaled boundary finite element method, Computer Methods in Applied Mechanics and Engineering 376 (2021) 113665. DOI: <https://doi.org/10.1016/j.cma.2021.113665>
- [9] N. Wattanasakulpong, V. Ungbhakorn, Linear and nonlinear vibration analysis of elastically restrained ends FGM beams with porosities, Aerospace Science and Technology 32/1 (2014) 111-120. DOI: <https://doi.org/10.1016/j.ast.2013.12.002>

- [10] J. Zhao, Q. Wang, X. Deng, K. Choe, R. Zhong, C. Shuai, Free vibrations of a functionally graded porous rectangular plate with uniform elastic boundary conditions, *Composites Part B: Engineering* 168 (2019) 106-120. DOI: <https://doi.org/10.1016/j.compositesb.2018.12.044>
- [11] B. Mechab, I. Mechab, S. Benaissa, M. Ameri, B. Serier, Probabilistic analysis of effect of the porosities in functionally graded material nanoplate resting on Winkler–Pasternak elastic foundations, *Applied Mathematical Modelling* 40/2 (2016) 738-749. DOI: <https://doi.org/10.1016/j.apm.2015.09.093>
- [12] Y.Q. Wang, J.W. Zu, Vibration behaviors of functionally graded rectangular plates with porosities and moving in thermal environment, *Aerospace Science and Technology* 69 (2017) 550-562. DOI: <https://doi.org/10.1016/j.ast.2017.07.023>
- [13] F.Z. Jouneghani, R. Dimitri, M. Baccocchi, F. Tornabene, Free Vibration Analysis of Functionally Graded Porous Doubly-Curved Shells Based on the First-Order Shear Deformation Theory, *Applied Sciences* 7/12 (2017) 1252. DOI: <https://doi.org/10.3390/app7121252>
- [14] P. Tossapanon, N. Wattanasakulpong, Flexural vibration analysis of functionally graded sandwich plates resting on elastic foundation with arbitrary boundary conditions: Chebyshev collocation technique, *Journal of Sandwich Structures and Materials* 22/2 (2020) 156-189. DOI: <https://doi.org/10.1177/1099636217736003>
- [15] H.A. Atmane, A. Tounsi, F. Bernard, Effect of thickness stretching and porosity on mechanical response of a functionally graded beams resting on elastic foundations, *International Journal of Mechanics and Materials in Design* 13 (2017) 71-84. DOI: <https://doi.org/10.1007/s10999-015-9318-x>
- [16] N. Wattanasakulpong, A. Chaikittiratan, S. Pornpeerakeat, Vibration of size-dependent functionally graded sandwich microbeams with different boundary conditions based on the modified couple stress theory, *Journal of Sandwich Structures and Materials* 22/2 (2020) 220-247. DOI: <https://doi.org/10.1177/1099636217738909>
- [17] X.Y. Zhang, G. Fang, S. LeeFlang, A.A. Zadpoor, J. Zhou, Topological design, permeability and mechanical behavior of additively manufactured functionally graded porous metallic biomaterial, *Acta Biomaterialia* 84 (2018) 437-452. DOI: <https://doi.org/10.1016/j.actbio.2018.12.013>
- [18] Y.H. Dong, Y.H. Li, D. Chen, J. Yang, Vibration characteristics of functionally graded graphene reinforced porous nanocomposite cylindrical shells with spinning motion, *Composites Part B: Engineering* 145 (2018) 1-13. DOI: <https://doi.org/10.1016/j.compositesb.2018.03.009>
- [19] T.V. Liena, N.T. Duc, N.T. Khiem, Free and forced vibration analysis of multiple cracked FGM multi-span continuous beams using dynamic stiffness method, *Latin American Journal of Solids and Structures* 16/2 (2018) e157. DOI: <http://dx.doi.org/10.1590/1679-78255242>
- [20] S. Hayat, S. Meriem, Vibration analysis of functionally graded plates with porosity composed of a mixture of Aluminum (Al) and Alumina ( $Al_2O_3$ ) embedded in an elastic medium, *Frattura ed Integrità Strutturale* 13/50 (2019) 286-299. DOI: <https://doi.org/10.3221/IGF-ESIS.50.24>
- [21] V.N. Burlayenko, T. Sadowski, Free vibrations and static analysis of functionally graded sandwich plates with three-dimensional finite elements, *Meccanica* 55 (2020) 815-832. DOI: <https://doi.org/10.1007/s11012-019-01001-7>
- [22] A.F. Mota, M.A.R. Loja, Mechanical Behavior of Porous Functionally Graded Nanocomposite Materials, *Journal of Carbon Research* 5/2 (2019) 34. DOI: <https://doi.org/10.3390/c5020034>
- [23] Y. Zhang, G. Jin, M. Chen, T. Ye, C. Yang, Y. Yin, Free vibration and damping analysis of porous functionally graded sandwich plates with a viscoelastic core, *Composite Structure* 244 (2020) 112298. DOI: <https://doi.org/10.1016/j.compstruct.2020.112298>
- [24] R. Bennai, H. Fourn, A.A. Hassen, A. Tounsi, Dynamic and wave propagation investigation of FGM plates with porosities using a four-variable plate theory, *Wind and Structures* 28/1 (2019) 49-62. DOI: <http://dx.doi.org/10.12989/was.2019.28.1.049>
- [25] V.N. Van Do, A Modified Kirchhoff plate theory for Free Vibration analysis of functionally graded material plates using meshfree method, *IOP Conference Series: Earth and Environmental Science* 143 (2018) 012038. DOI: <https://doi.org/10.1088/1755-1315/143/1/012038>
- [26] C.M. Wang, S. Kitipornchai, J.N. Reddy, Relationship between vibration frequencies of Reddy and Kirchhoff polygonal plates with simply supported edges, *Journal of Vibration and Acoustics* 122/1 (2000) 77-81. DOI: <https://doi.org/10.1115/1.568438>
- [27] C.M Wang, J.N. Reddy, K.H. Lee, *Shear Deformable Beams and plates Relationships with Classical Solutions*, First Edition, Elsevier Science, 2000. DOI: <https://doi.org/10.1016/B978-0-08-043784-2.X5000-X>
- [28] S.J. Singh, S.P. Harsha, Thermo-mechanical analysis of porous sandwich S-FGM plate for different boundary

- conditions using Galerkin Vlasov's method: a semi-analytical approach, *Thin-Walled Structures* 150 (2020) 106668. DOI: <https://doi.org/10.1016/j.tws.2020.106668>
- [29] N. Wattanasakulpong, A. Chaikittiratana, Flexural vibration of imperfect functionally graded beams based on Timoshenko beam theory, Chebyshev collocation method, *Meccanica* 50 (2015) 1331-1342. DOI: <https://doi.org/10.1007/s11012-014-0094-8>
- [30] S. Chakraverty, K.K. Pradhan, Free Vibration of exponential functionally graded rectangular plates in thermal environment with general boundary conditions, *Aerospace Science and Technology* 36 (2014) 132-156. DOI: <https://doi.org/10.1016/j.ast.2014.04.005>
- [31] S.S. Rao, *The Finite Element Method in Engineering*, Sixth Edition, Elsevier Inc., 2018.
- [32] N.V. Nguyen, H.N. Xuan, D. Lee, J. Lee, A novel computational approach to functionally graded porous plates with graphene platelets reinforcement, *Thin-Walled Structures* 150 (2020) 106684. DOI: <https://doi.org/10.1016/j.tws.2020.106684>
- [33] C. Li, H.S. Shen, H. Wang, Z. Yu, Large amplitude vibration of sandwich plates with functionally graded auxetic 3D lattice core, *International Journal of Mechanical Sciences* 174 (2020) 105472. DOI: <https://doi.org/10.1016/j.ijmecsci.2020.105472>
- [34] M.J. Jweeg, M. Al-Waily, A.A. Deli, Theoretical and Numerical Investigation of Buckling of Orthotropic Hyper Composite Plates, *International Journal of Mechanical and Mechatronics Engineering* 15/4 (2015) 1-12.
- [35] M. Al-Waily, A.A. Deli, A.D. Al-Mawash, Z.A.A. Abud Ali, Effect of Natural Sisal Fiber Reinforcement on the Composite Plate Buckling Behavior, *International Journal of Mechanical and Mechatronics Engineering* 17/1 (2017) 30-37.
- [36] S.M. Abbas, A.M. Takhakh, M.A. Al-Shammari, M. Al-Waily, Manufacturing and Analysis of Ankle Disarticulation Prosthetic Socket (SYMES), *International Journal of Mechanical Engineering and Technology* 9/7 (2018) 560-569.
- [37] J.S. Chiad, M. Al-Waily, M.A. Al-Shammari, Buckling Investigation of Isotropic Composite Plate Reinforced by Different Types of Powders, *International Journal of Mechanical Engineering and Technology* 9/9 (2018) 305-317.
- [38] E.N. Abbas, M.J. Jweeg, M. Al-Waily, Analytical and Numerical Investigations for Dynamic Response of Composite Plates Under Various Dynamic Loading with the Influence of Carbon Multi-Wall Tube Nano Materials, *International Journal of Mechanical and Mechatronics Engineering* 18/6 (2018) 1-10.
- [39] M. Al-Waily, M.A. Al-Shammari, M.J. Jweeg, An Analytical Investigation of Thermal Buckling Behavior of Composite Plates Reinforced by Carbon Nano Particles, *Engineering Journal* 24/3 (2020) 11-21. DOI: <https://doi.org/10.4186/ej.2020.24.3.11>
- [40] M. Al-Waily, M.H. Tolephih, M.J. Jweeg, Fatigue Characterization for Composite Materials used in Artificial Socket Prostheses with the Adding of Nanoparticles, *IOP Conference Series: Materials Science and Engineering* 928 (2020) 022107. DOI: <https://doi.org/10.1088/1757-899X/928/2/022107>
- [41] E.K. Njim, S.H. Bakhy, M. Al-Waily, Optimization design of vibration characterizations for functionally graded porous metal sandwich plate structure, *Materials Today: Proceedings* (2021) (in press). DOI: <https://doi.org/10.1016/j.matpr.2021.03.235>
- [42] E.K. Njim, M. Al-Waily, S.H. Bakhy, A Review of the Recent Research on the Experimental Tests of Functionally Graded Sandwich Panels, *Journal of Mechanical Engineering Research and Developments* 44/3 (2021) 420-441.
- [43] M.J. Jweeg, A.S. Hammood, M. Al-Waily, A suggested analytical solution of Isotropic composite plate with crack effect, *International Journal of Mechanical and Mechatronics Engineering* 12/5 (2012) 44-58.
- [44] M. Al-Waily, Z.A.A. Abud Ali, A suggested analytical solution of powder reinforcement effect on buckling load for isotropic mat and short hyper composite materials plate, *International Journal of Mechanical and Mechatronics Engineering* 15/4 (2015) 80-95.
- [45] M. Al-Waily, K.K. Resan, A.H. Al-Wazir, Z.A.A. Abud Ali, Influences of Glass and Carbon Powder Reinforcement on the Vibration Response and Characterization of an Isotropic Hyper Composite Materials Plate Structure, *International Journal of Mechanical and Mechatronics Engineering* 17/6 (2017) 74-85.
- [46] M.A. Al-Shammari, M. Al-Waily, Analytical Investigation of Buckling Behavior of Honeycombs Sandwich Combined Plate Structure, *International Journal of Mechanical and Production Engineering Research and Development* 8/4 (2018) 771-786. DOI: <http://dx.doi.org/10.24247/ijmperdaug201883>
- [47] M.R. Ismail, Z.A.A. Abud Ali, M. Al-Waily, Delamination Damage Effect on Buckling Behavior of Woven Reinforcement Composite Materials Plate, *International Journal of Mechanical and Mechatronics Engineering* 18/5 (2018) 83-93.
- [48] H.J. Abbas, M.J. Jweeg, M. Al-Waily, A.A. Diwan, Experimental Testing and Theoretical Prediction of Fiber Optical Cable for Fault Detection and

- Identification, *Journal of Engineering and Applied Sciences* 14/2 (2019) 430-438.  
DOI: <http://dx.doi.org/10.36478/jeasci.2019.430.438>
- [49] E.N. Abbas, M.J. Jweeg, M. Al-Waily, Fatigue Characterization of Laminated Composites used in Prosthetic Sockets Manufacturing, *Journal of Mechanical Engineering Research and Developments* 43/5 (2020) 384-399.
- [50] E.K. Njim, S.H. Bakhy, M. Al-Waily, Analytical and numerical investigation of buckling load of functionally graded materials with porous metal of sandwich plate, *Materials Today: Proceedings* (2021) (in press).  
DOI: <https://doi.org/10.1016/j.matpr.2021.03.557>
- [51] M.A. Al-Shammari, M. Al-Waily, Theoretical and numerical vibration investigation study of orthotropic hyper composite plate structure, *International Journal of Mechanical and Mechatronics Engineering* 14/6 (2014) 1-21.
- [52] A.A. Alhumdany, M. Al-Waily, M.H.K. Al-Jabery, Theoretical and Experimental Investigation of Using Date Palm Nuts Powder into Mechanical Properties and Fundamental Natural Frequencies of Hyper Composite Plate, *International Journal of Mechanical and Mechatronics Engineering* 16/1 (2016) 70-80.
- [53] A.A. Kadhim, M. Al-Waily, Z.A.A. Abud Ali, M.J. Jweeg, K.K. Resan, Improvement Fatigue Life and Strength of Isotropic Hyper Composite Materials by Reinforcement with Different Powder Materials, *International Journal of Mechanical and Mechatronics Engineering* 18/2 (2018) 77-86.
- [54] S.M. Abbas, K.K. Resan, A.K. Muhammad, M. Al-Waily, Mechanical and fatigue behaviors of prosthetic for partial foot amputation with various composite materials types effect, *International Journal of Mechanical Engineering and Technology* 9/9 (2018) 1-8.
- [55] M.J. Jweeg, M. Al-Waily, A.K. Muhammad, K.K. Resan, Effects of Temperature on the Characterisation of a New Design for a Non-Articulated Prosthetic Foot, *IOP Conference Series: Materials Science and Engineering* 433 (2018) 012064. DOI: <https://doi.org/10.1088/1757-899X/433/1/012064>
- [56] M.A. Al-Shammari, Q.H. Bader, M. Al-Waily, A.M. Hasson, Fatigue Behavior of Steel Beam Coated with Nanoparticles under High Temperature, *Journal of Mechanical Engineering Research and Developments* 43/4 (2020) 287-298.
- [57] E.N. Abbas, M. Al-Waily, T.M. Hammza, M.J. Jweeg, An Investigation to the Effects of Impact Strength on Laminated Notched Composites used in Prosthetic Sockets Manufacturing, *IOP Conference Series: Materials Science and Engineering* 928 (2020) 022081. DOI: <https://doi.org/10.1088/1757-899X/928/2/022081>
- [58] S.E. Sadiq, M.J. Jweeg, S.H. Bakhy, The Effects of Honeycomb Parameters on Transient Response of an Aircraft Sandwich Panel Structure, *IOP Conference Series: Materials Science and Engineering* 928 (2020) 022126. DOI: <https://doi.org/10.1088/1757-899X/928/2/022126>
- [59] Z.A.A. Abud Ali, A.A. Kadhim, R.H. Al-Khayat, M. Al-Waily, Review Influence of Loads upon Delamination Buckling in Composite Structures, *Journal of Mechanical Engineering Research and Developments* 44/3 (2021) 392-406.
- [60] A.A. Kadhim, E.A. Abbod, A.K. Muhammad, K.K. Resan, M. Al-Waily, Manufacturing, and Analyzing of a New Prosthetic Shank with Adapters by 3D Printer, *Journal of Mechanical Engineering Research and Developments* 44/3 (2021) 383-391.



© 2021 by the authors. Licensee International OCSCO World Press, Gliwice, Poland. This paper is an open access paper distributed under the terms and conditions of the Creative Commons Attribution-NonCommercial-NoDerivatives 4.0 International (CC BY-NC-ND 4.0) license (<https://creativecommons.org/licenses/by-nc-nd/4.0/deed.en>).